BMC Medical Genomics

RESEARCH

Open Access

# Exploring diagnostic m6A regulators in primary open-angle glaucoma: insight from gene signature and possible mechanisms by which key genes function

Xinyue Zhang[1,2†], Jiawei Chen[1,2†], Xiaoyu Zhou[1,2], Dengming Zhou[3], Li Liao[2], Yang Zhao[1], Ping Wu[2], Fen Nie[1], Zhimin Liao[1], Ziyan Cai[4] and Xuanchu Duan[1,2*]

## Abstract

**Purpose** The purpose of this study was to interrogate the potential role of N6-methyladenosine (m6A) regulators in the process of trabecular meshwork (TM) tissue damage in patients with primary open-angle glaucoma (POAG).

**Methods** Firstly, the expression profile of m6A regulators in TM tissues of POAG patients was comprehensively analyzed by bioinformatics analysis; Plasmid transfection and siRNA gene interference were used to enhance or weaken the expression levels of YTHDC2 in human trabecular meshwork cells (HTMCs); Cell migration ability was detected by transwell chamber assay; Immunofluorescence staining assay was used to evaluate the expression of extracellular matrix (ECM) related proteins.

**Results** Through the analysis of GSE27276 database, 5 m6A regulators with different expression in POAG were screened out. The results of random forest model showed that these 5 m6A regulators exhibited diagnostic potential and were characteristic genes of POAG. All POAG samples could be effectively divided into two groups based on the expression levels of these 5 hub m6A regulators. Immune cell infiltration analysis indicated that the levels of activated $CD8^+$ T cells and regulatory T cells were different in the two subtypes. HTMC oxidative stress cell model and TGF-β2 stimulation cell model were further constructed to verify the expression of the aforementioned hub m6A regulators, and it was found that YTHDC2 mRNA showed the same expression trend in both models. The silencing of YTHDC2 enhanced the migration ability of HTMCs and increased the synthesis ability of ECM. However, when $YTHDC2^{\Delta YTH}$, which lacks the YTH domain, is overexpressed in HTMCs, there is no significant change in the ECM synthesis ability.

**Conclusions** The differentially expressed m6A regulators in TM tissues may serve as potential diagnostic biomarkers for POAG. And, in HTMCs, the expression level of YTHDC2 mRNA was changed under oxidative stress or TGF-β2 intervention, and then exerted its regulation on cell migration and ECM synthesis capability through m6A modification, which may be an important part of the disease process of POAG.

**Keywords** Glaucoma, POAG, N6-methyladenosine, Trabecular meshwork, Oxidative stress

†Xinyue Zhang and Jiawei Chen contributed equally.

*Correspondence:
Xuanchu Duan
duanxchu@csu.edu.cn
Full list of author information is available at the end of the article

## Introduction

Glaucoma is characterized by optic nerve damage with characteristic visual field impairment. According to statistics, it is the main cause of permanent vision impairment [1]. More than 100 million people are expected to suffer from glaucoma by 2040 [2]. Primary open-angle glaucoma (POAG) is the most common type, accounting for about 74% of all glaucoma patients [2]. Its pathogenesis is complex, still unclear, and there is no radical cure, which is still a huge challenge for medical workers. In the current study, elevated intraocular pressure (IOP) is the only treatable risk factor for POAG [3]. The balance between the secretion and outflow of aqueous humor has important physiological significance for maintaining normal IOP [4]. Aqueous humor in the human eye is mainly filtered through the trabecular meshwork (TM), a filter-like structure located in the angle of the anterior chamber. Therefore, TM dysfunction will reduce aqueous humor drainage, leading to ocular hypertension and further induce POAG [5]. The treatment method to restore the function of TM is the closest to restore the aqueous humor circulation in physiological state, which is more consistent with clinical needs in reducing IOP and preventing functional vision loss, and is an important area of research. However, currently approved drugs for the treatment of glaucoma do not specifically target TM. Therefore, the mechanism of TM dysfunction in POAG needs to be further explored, which is conducive to the development of targeted drugs to repair TM function.

More and more scholars began to focus on the role of epigenetic regulation in POAG, such as methylation, histone acetylation, non-coding RNA, etc. [6–8]. However, it has to be said that the epigenetic mechanisms and therapies in maintaining the aqueous humor outflow remain to be defined. N6-methyladenosine (m6A) RNA modification is the most conserved and predominant internal mRNA modification found in current studies. It is one of the important ways to achieve the post-transcriptional regulation of gene expression [9]. Three key regulatory factors are required for the regulation of M6A modification: m6A methyltransferases (such as RBM15/15B, WTAP, METTL3, METTL14 and VIRMA), demethylases (such as ALKBH5 and FTO) and m6A binding proteins (such as IGF2BP1/2/3, HNRNPC, YTHDC1/2, and YTHDF1/2/3). M6A methyltransferases catalyze m6A, and it can be reversed by demethylases to achieve homeostasis [10]. In addition, the m6A binding protein can bind to the m6A modification site in RNA and affect target genes expression by regulating RNA transcription, cleavage, maturation, stability, translation, etc. [11]. Recent studies have identified that m6A modification can regulate various biological processes such as cell proliferation, T cell homeostasis and differentiation, antiviral, anti-tumor immune response, and anti-inflammatory response [12]. Thus, m6A modification plays a significant role in the pathogenesis of various neoplastic or non-neoplastic diseases [13, 14], but has rarely been studied in glaucoma. Niu et al. [15] found that YTHDF2, a m6A binding protein, is highly expressed in the mouse RGCs. This study showed that YTHDF2 inhibited RGC dendrite development and suggested that YTHDF2 and its target mRNAs might be potential therapeutic targets for glaucoma.

This study aims to comprehensively explore the unique pattern of m6A regulators in the TM of POAG patients from the perspective of bioinformatics, and conduct preliminary verification through cell experiments, in order to provide new insights for the study of the pathogenesis of POAG.

## Materials and methods

### Data resources and preprocessing

Retrieve POAG-related data sets through the Gene Expression Omnibus (GEO) database. The following keywords were used for the initial screen: "primary open-angle glaucoma" or "POAG" and "trabecular meshwork" with "homo sapiens" or "human". Two candidate datasets: GSE27276 [16] (platform: GPL2507) and GSE4316 [17] (platform: GPL570) were identified after searching. In order to reduce the "platform effect", GSE27276 was reserved to perform bioinformatics analysis at last.

Probes were annotated according to the GPL2507 annotation file. Then, the genome-wide expression profile was normalized through the corresponding R package.

### The expression landscape of m6A regulators in POAG

Following pretreatment, the "limma package" was used to identify differentially expressed m6A regulators in the contrasting matrices: normal vs. POAG based on R software (R version 4.1.3). Then "ggpubr" package was used to draw a boxplot in order to show the expression landscape of these regulators. In addition, a heatmap was drawn using the "pheatmap" package in R. Spearman's correlation analysis was used to determine the correlations between the m6A regulator expression levels and POAG.

### Screening the disease characteristic genes

To obtain more accurate POAG signature genes, the "randomForest" and "kernlab" R package were utilized respectively to build random forest tree model and machine learning model. The reverse cumulative distribution of residual plot was drawn using the "DALEX" package in R. Additionally, the "ggplot2" R package was used to draw the boxplot of residual. ROC curve analysis was performed using the "pROC" package. The lower the

residual value, the larger the area under the curve (AUC), the higher the accuracy of the model. Then select a more appropriate model for the next step of analysis. The "randomForest" R package was applied to evaluate the significance of m6A regulators in POAG [18]. Genes with gene importance score greater than 2 were selected for subsequent analysis, and the corresponding gene importance score plot was drawn.

Firstly, the selected disease characteristic genes were used to construct the model. The "rms" package was used to draw a nomogram and the corresponding Calibration curve. In addition, the "rmda" package was used to carry out the Decision Curve Analysis (DCA) and draw the Clinical Impact Curve further. The Calibration curve, DCA and Clinical Impact Curve were all used for model evaluation.

#### Sample clustering analysis

Clustering analysis was carried out for the identified m6A regulators. In order to clarify the sum of clusters, "ConsensusClusterPlus" R package was used for consensus clustering through resampling iteration (maxK = 9) [19]. Use the "pheatmap" package to draw the corresponding heatmap. Then the "limma package" was used to identify differentially expressed m6A regulators in the contrasting m6Acluster subtypes: A vs. B with a threshold of $p < 0.05$. The boxplot was drawn with the "ggpubr" R package to show the expression pattern of the selected m6A regulators. Moreover, a heatmap was drawn using the "pheatmap" package in R. Moreover, the principal components analysis (PCA) was carried out to evaluate the cluster distribution of m6A clustering, and the "ggplot2" package was utilized for visualization. Then the "limma package" was used to identify differentially expressed genes (DEGs) between the m6Acluster subtype A and B with a threshold of adj.P.Val.Filter < 0.05 and |logFC| < 0.5. And then, in the same way, these DEGs were used to sub-classify the POAG samples. In addition, the PCA was used to score each POAG sample according to the expression levels of m6A-related genes, and then the m6A score results of each sample were obtained. The "limma" package was then used for comparison between groups and the result was demonstrated in a boxplot using "ggpubr" package. Finally, the Sankey diagram was drawn through "ggalluvial" package to compare the results of the two types of clustering and the m6A scores.

#### The association between m6A regulators and infiltrating immune cells in POAG

Single-sample gene set enrichment analysis (ssGSEA) was performed using the "GSVA" package to evaluate the correlation between m6A regulators and infiltrating immune cells in TM tissues of POAG patients [20][20]. Different types of immune cells are labeled by a series of different marker genes, which are collated in a ".gmt" file as the reference gene set. The ssGSEA enrichment scores of these immune cells were then scaled and compared between the m6Acluster subtype A and m6Acluster subtype B (or genecluster subtype A and genecluster subtype B), and the association of m6A regulators with infiltrating immune cells was assessed by Spearman correlation analysis.

#### Functional enrichment analyses

Gene Ontology (GO) analysis, including molecular function (MF), biologic process (BP), and cellular components (CC), was realized by the "ClusterProfiler" package.

#### Culture of primary human trabecular meshwork cells

Primary human trabecular meshwork cells (HTMCs) were isolated from non-glaucomatous donor tissue rings by the tissue mass culture method [21]. All human tissue specimens were obtained in accordance with the corresponding guiding principles of the Declaration of Helsinki. The TM tissues we used for primary culture was derived from the excess corneoscleral rings after corneal transplantation and were provided by the eye bank of Changsha Aier Eye Hospital. This study was approved by the ethics committee of Changsha Aier Eye Hospital (Ethics approval No. KYPJ0010). The cell complete medium was formulated as follows: 89% DMEM/F12, 10% fetal bovine serum (Gibco) and 1% penicillin/streptomycin solution (Gibco). The passage of any validated TM cells should be within 4–6 to retain the primary phenotypes.

TGF-β2 was purchased from Peprotech. Before the treatment, the solution with a final concentration of 5 ng/ml in serum-free medium was prepared. The 5 ng/ml TGF-β2 was introduced in the HTMCs and incubated for 72 h. After the duration time, the TGF-β2 treatment was stopped with phosphate-buffered saline (PBS, Gibco) washing for further cell function test or RNA extraction. 30% Hydrogen peroxide ($H_2O_2$) was purchased from Sigma-Aldrich. The reagent was diluted to different concentrations in serum-free medium by a stepwise dilution method. After the appropriate time, the $H_2O_2$ intervention was stopped with twice PBS washing, and further followed by RNA extraction.

#### Cell transfection

The over-expression plasmids of wild-type YTHDC2 ($YTHDC2^{WT}$), mutant YTHDC2 without YTH domain ($YTHDC2^{\Delta YTH}$) and their negative control (Empty) were all designed by RiboBio. The HTMCs ($4 \times 10^4$) were inoculated into a six-well plate prior to transfection. Transfection was performed using Lipofectamine 3000 (Life Technologies) according to the manufacturer's

instructions. Cells were incubated for 24–48 h after transfection before further experiments were performed.

#### RNA extraction and quantitative reverse-transcription polymerase chain reaction

Total RNA extraction was performed using Trizol Reagent (Invitrogen). The extracted RNA was dissolved in RNase Free dH2O. Next, the genomic DNA elimination step was first performed using 4×gDNA wiper Mix (Vazyme) reagent and incubated at 42 °C for 2 min. Then, first-strand cDNA was synthesized using the 5×HiScriptII qRT SuperMix II(Vazyme). Polymerase chain reaction (PCR) for m6A-related genes was performed using ChamQ Universal SYBR qPCR Master Mix (Vazyme). The relative expression levels of m6A-related genes were normalized to GAPDH or beta-actin. The primers were designed by RiboBio. The relative folding changes of m6A regulators were determined by the $2^{-\Delta\Delta Ct}$ method.

#### Immunofluorescence staining

The cells were fixed with methanol at room temperature for 10 min and washed 3 times with PBS. Then, the HTMCs were blocked by 5% bovine serum albumin (Biosharp) for 1 h. After washing with PBS 3 times, add the primary antibody diluted in PBS at a ratio of 1:100, and incubate at 4 °C overnight. The primary antibodies used were as follows: Collagen I (COL1A1, ZEN-BIOSCIENCE, R26615, monoclonal antibody), Smooth Muscle Actin (ASMA, SANTA CRUZ, sc-53142, monoclonal antibody) and Fibronectin (FN, SANTA CRUZ, sc-8422, monoclonal antibody). The next day, after washing the cells 3 more times, the secondary antibody (Alexa Fluro 488, SANTA CRUZ) was added and incubated at room temperature for 1 h. Similarly, after washing the cells for 3 times, DAPI (Biosharp) was added to stain the cells for 1 min. After PBS washing, anti-fluorescence quencher (Solarbio) was added and the images was obtained by Nikon fluorescence microscope.

#### *Cell migration assays*

Cell migration ability was examined by the transwell assay. After digestion, the HTMCs ($4\times10^4$) were resuspended with 250 µl serum-free medium and then implanted in the upper chamber of the 24-well transwell plate (Corning). 750 µl medium containing 10% FBS was added to the lower chamber. After incubation for 36 h, in order to assess the number of cells migrating to the lower surface of the membrane, the chambers were first impregnated with methanol at room temperature for 30 min to complete cell fixation, and then stained with crystal violet after PBS washing. Images are obtained with Nikon microscop and quantified with ImageJ software.

#### Statistics analysis

R software (version 4.1.3) was used for bioinformatics analysis. SPSS software (version 22.0) and GraphPad Prism software (version 9.0) were used for statistical analysis and plotting. Continuous data were summarized as mean ± standard deviation. Student's t-test and analysis of variance were used to examine differences in continuous variables. All in vitro experiments were performed at least three technical and biological replicates. The $p$ value < 0.05 was considered statistically significant.

## Results

#### The mRNA expression landscape of m6A regulators in POAG

More and more m6A regulators have been identified. First, the expression levels of 25 m6A regulators between human TM tissue of normal subjects and those of patients with POAG was scrutinized and compared. Data of 19 normal, 17 POAG samples of TM tissues were acquired from the GEO database (GSE27276) and these samples were used to determine the expression levels of m6A regulators in POAG. The expression patterns of these m6A regulators were shown in Fig. 1A. Of the 25 m6A regulators, 5 showed significant differences in expression between the two groups, including RBM15, YTHDC2, YTHDF1, RBMX and ALKBH5. The heatmap further showed the expression of the 5 m6A regulators in the normal and POAG samples (Fig. 1B). This suggested their possible participation in development of POAG. Correlation analysis showed that the positive correlation coefficient between FTO and YTHDC1 was the highest (r = 0.68), the negative correlation coefficient between YTHDF2 and ALKBH5 was the highest (r = −0.6) (Fig. 1C). The relative positions of these regulators on chromosomes were shown in Fig. 1D.

#### Screening of the m6A-associated characteristic genes of POAG

In order to more accurately screen the characteristic genes of POAG, model selection was carried out first. The Random Forest (RF) model and Support Vector Machine (SVM) model were established respectively and the corresponding boxplots of |residual|, reverse cumulative distribution of |residual| and ROC curve analysis were drawn (Figs. 2A-C). The results showed that the |residual| of the RF model was lower, and the area under the ROC curve (AUC) was larger, indicating that the RF model was more precise. Subsequently, the RF model was selected to screen the disease characteristic genes. Find the point with the minimum cross-validation error, the number of trees corresponding to this point is the optimal number of trees (Fig. 2D), and then draw gene importance scores diagram (Fig. 2E). The results showed

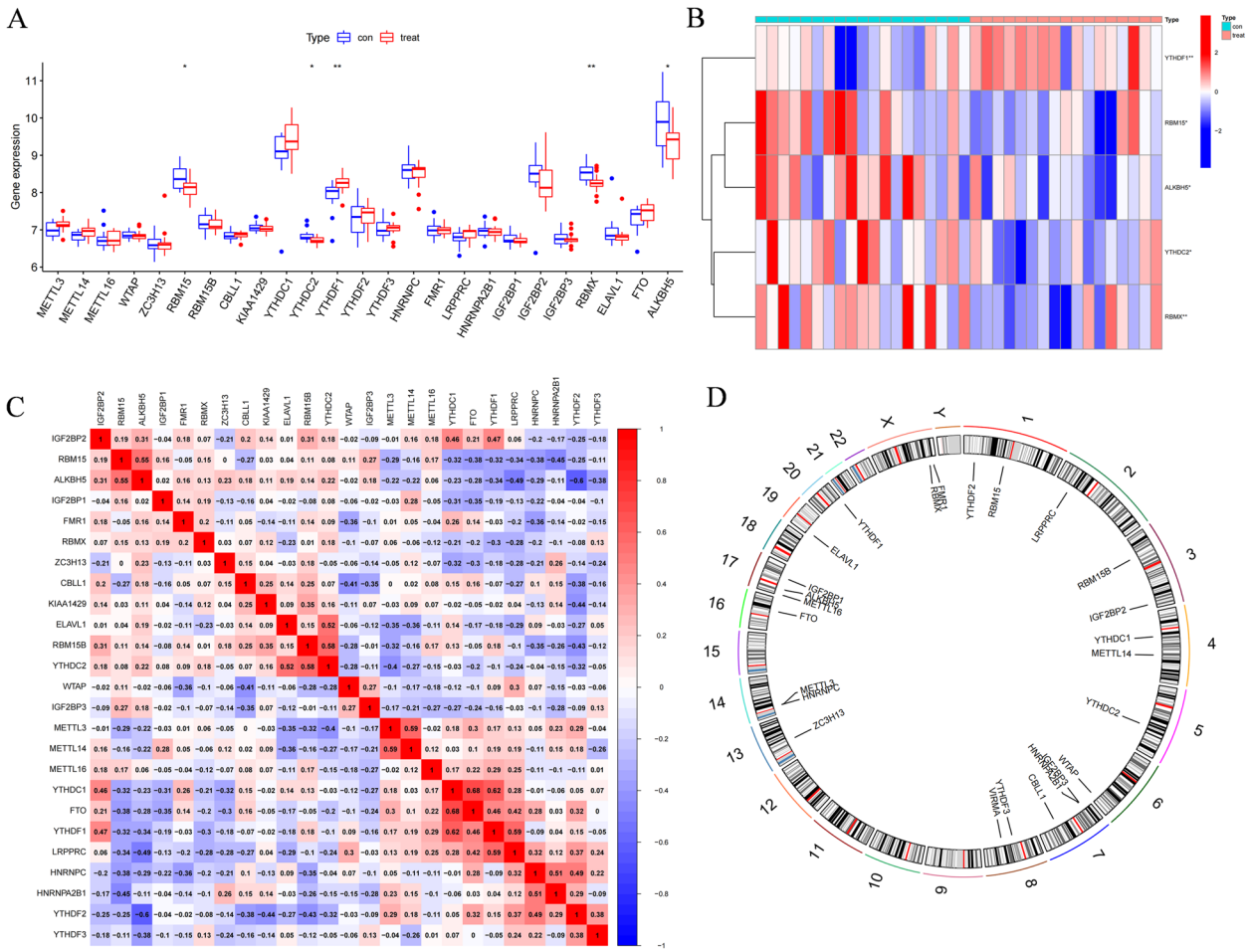


**Fig. 1** The mRNA expression landscape of 25 m6A regulators in POAG. **A** Boxplot showing 5 m6A regulators with significant difference in their RNA expression between normal and POAG samples. **B** The heatmap of 5 differentially expressed m6A regulators' expression among normal and POAG samples. **C** Spearman correlation analysis of 25 m6A regulators expression in TM. (D)The relative positions of the 25 m6A regulators on chromosomes.* $p < 0.05$; ** $p < 0.01$

that the scores of the five differentially expressed m6A regulators were all over 2, suggesting that all of them may play a part in regulating the function of TM. Genes with gene importance score > 2 were selected for subsequent analysis.

### The generation and evaluation of nomogram based on m6A genes

Based on gene importance score > 2, five important genes were determined, which are YTHDF1, RBMX, ALKBH5, YTHDC2 and RBM15. The nomogram was drawn with these 5 m6A genes, as shown in Fig. 3A. The individual score of each gene can be obtained according to the expression levels of these 5 m6A regulators in a patient. Then, summing the scores of all genes can get the comprehensive score of the patient and realize the prediction of the risk of POAG. In addition, the model was evaluated using three different methods respectively (Figs. 3B-D), showing that the model has a high accuracy. These results demonstrated the successful establishment of nomogram based on m6A genes for predicting risk of POAG.

### Determine m6A regulator subtype

The mRNA expression of the 5 hub m6A regulators were applied to consensus clustering analysis for different POAG samples in R with the β-values of probes. The results showed that when $k = 9$ gradually changed to $k = 2$, the clustering stability also gradually improved, so the result when $k = 2$ is optimal (Figs. 4A-B). Therefore, the POAG samples could be divided into two subtypes. The dark blue color displayed in the subtype indicated a strong correlation among samples within the group, while the white color was mainly displayed between groups, indicating a weak correlation between different subtypes (Fig. 4C). Therefore, it could be considered that the POAG samples were effectively divided into two

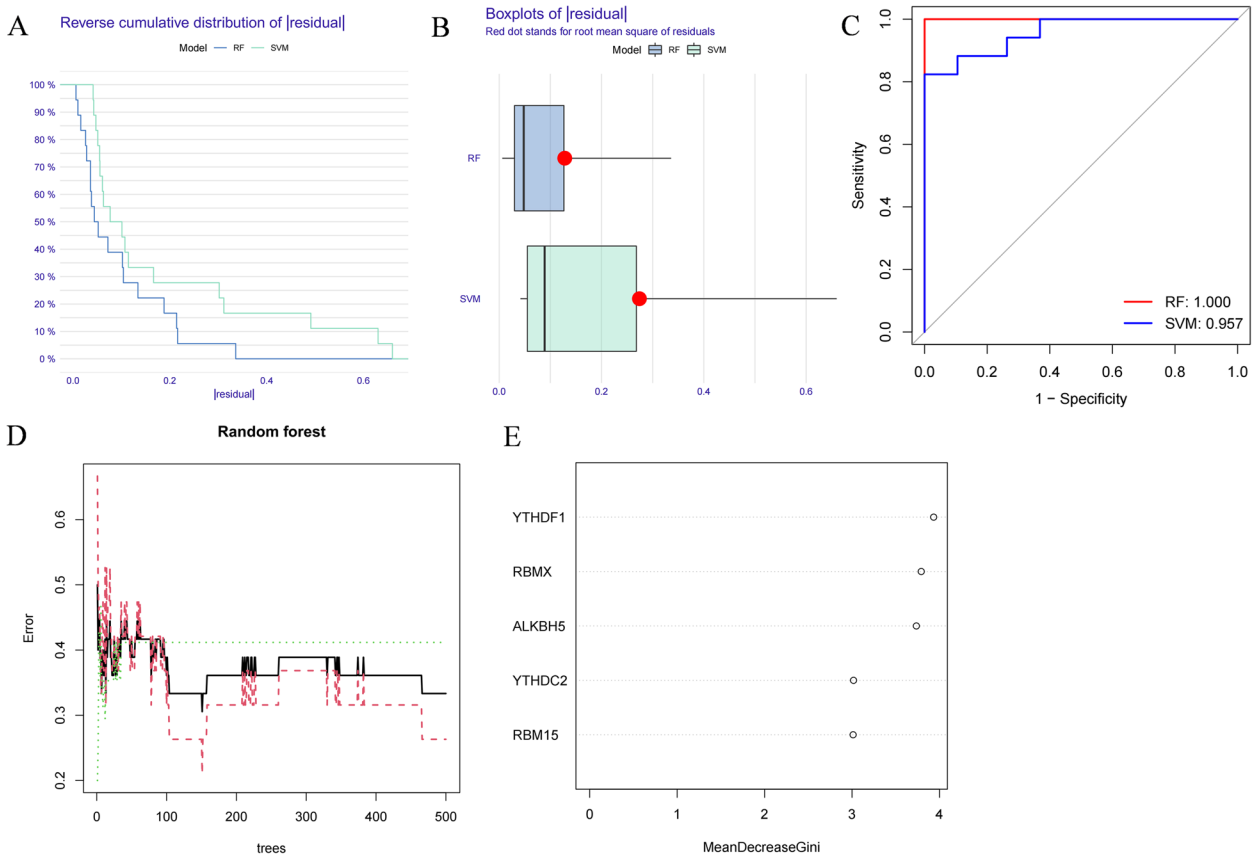


**Fig. 2** The m6A-associated characteristic genes of POAG. **A** The reverse cumulative distribution of |residual| and (**B**) Boxplots of |residual| showing a lower |residual| of the RF model. **C** ROC curve analysis of RF and SVM model showing a larger AUC of the RF model. **D**-**E** Random forest analysis ranking the importance of 5 m6A regulators in human TM tissue of patients with POAG based on their gene expression levels

groups. The expression landscape of 5 hub m6A regulators in the two different m6A subtypes was shown in Fig. 4D. The expression levels of RBM15, a m6A methyltransferase, and ALKBH5, a m6A demethylase, in m6Acluster subtype A were significantly higher than those in m6Acluster subtype B, while the expression of YTHDC2, YTHDF1 and RBMX were not significantly changed between the two different m6Acluster subtypes. The heatmap further showed the expression of the 5 m6A regulators in both the m6Acluster subtype A samples and m6Acluster subtype B samples (Fig. 4E). PCA analysis indicated that m6Acluster subtype A samples could be easily distinguished from m6Acluster subtype B samples (Fig. 4F).

### Immune cell infiltration analysis of the two different m6A subtypes

To further delve into the differences between the two groups, the infiltration of immune cells between the m6Acluster subtype A and B was compared. SsGSEA obtained the scores of immune cells in each sample, and the results indicated that activated $CD8^+$ T cell and regulatory T cell differed between the two different m6Acluster subtypes, and these two kinds of cells in m6Acluster subtype B was higher than those in subtype A (Fig. 5A). Correlation analysis of immune cells and m6A regulatory genes showed that the highest positive correlation coefficient was detected between activated $CD4^+$ T cell and RBM15 ($r=0.58$), the highest negative correlation coefficient was detected between activated $CD8^+$ T cell and ALKBH5 ($r=-0.61$) (Fig. 5B). The samples were further divided into two groups according to the expression levels of ALKBH5 and RBM15. It could be seen that the content of activated $CD8^+$ T cells was low in the high ALKBH5 expression group, while the content of activated $CD4^+$ T cells was high in the high RBM15 expression group, which was consistent with the above correlation analysis.

### Determine the landscape of gene subtype

To further explore the differences between the two subtypes, DEGs between the m6Acluster subtype A and B were identified with a threshold of adj.P.Val.Filter < 0.05 and |logFC| < 0.5. Subsequently, the results of GO

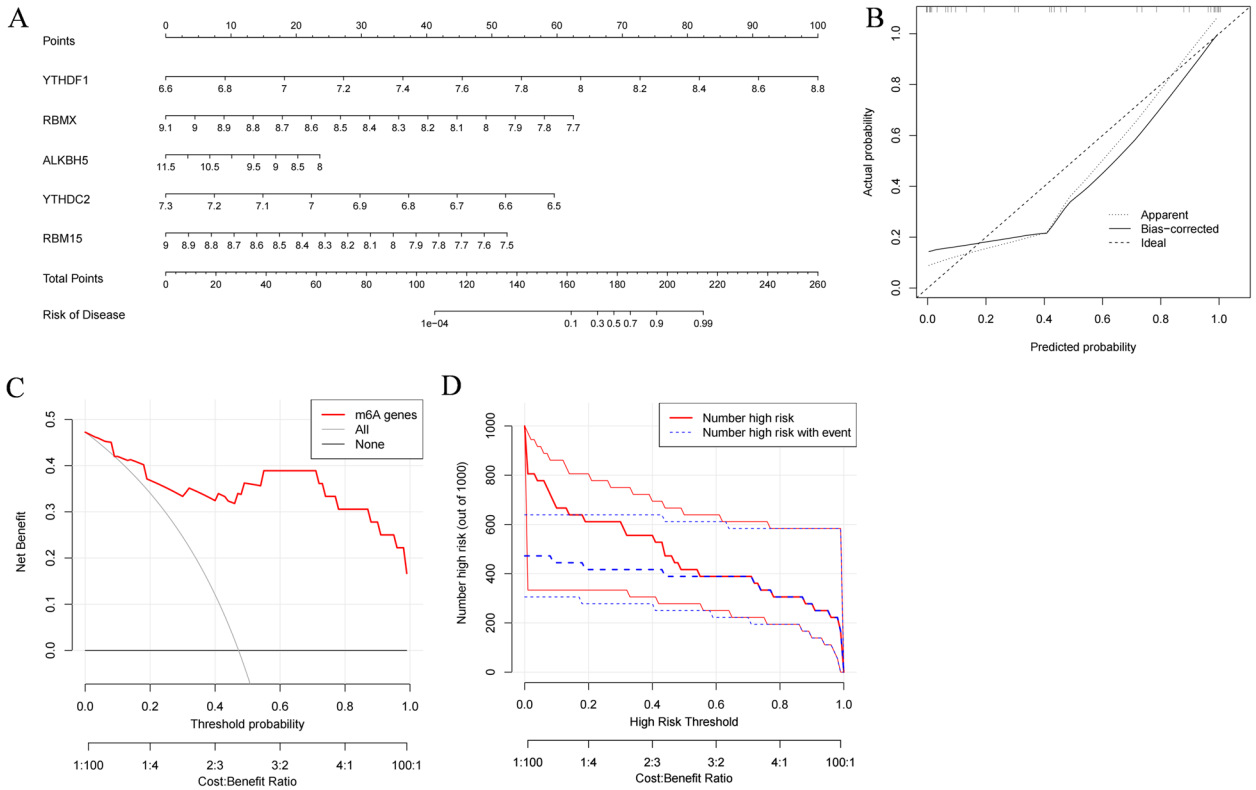


**Fig. 3** The generation and evaluation of nomogram for predicting the risk of POAG based on m6A genes (**A**) Nomogram to estimate a patient's risk of developing POAG. **B** Calibration curve analysis, (**C**) Decision Curve Analysis and (**D**) Clinical Impact Curve showing a high accuracy of the nomogram

enrichment analysis showed differences in gene expression between m6Acluster subtype A and B (Fig. 6A). These genes were involved in nucleobase-containing compound catabolic process, heterocycle catabolic process, cellular nitrogen compound catabolic process, oxidoreduction-driven active transmembrane transporter activity, primary active transmembrane transporter activity and so on. Subsequently, these DEGs were used to sub-classify the POAG samples in the same way. Of note, $k=2$ was also considered to be the optimal outcome (Fig. 6B). The expression of these regulators in the two different gene subtypes was shown in Fig. 6C. The same results seem to exist in gene clustering outcomes. To further decipher differences between the two geneCluster subtypes, the expression patterns of m6A regulators were compared. The results suggested that the expression of RBM15 and ALKBH5 in genecluster subtype A were significantly higher than those in genecluster subtype B, while the expression of YTHDC2, YTHDF1 and RBMX were not significantly different between the two different genecluster subtypes. The heatmap further showed the expression landscape of the 5 m6A regulators in both the genecluster subtype A samples and genecluster subtype B samples (Fig. 6D). In addition, immune cell infiltration of the two genecluster subtypes was also compared. The resulting profiles showed that the levels of activated $CD8^+$ T cell and regulatory T cell were both higher in genecluster subtype B than those in subtype A (Fig. 6E). Furthermore, according to the expression patterns of m6A regulators, the PCA method was used to score each sample to obtain the m6A score result. The results of the comparison between subtypes were demonstrated in the boxplots (Fig. 6F-G), which showed that there was no significant statistical difference in the m6A score between m6Acluster subtype A and B, and the same result was found between genecluster subtype A and B. Moreover, the Sankey diagram was drawn to compare the results of the two types of typing and the landscape of m6A score (Fig. 6H). It can be seen that the results of the m6Acluster subtype and the results of the genecluster subtype completely coincided, but in general, the m6A scores of most samples in all subtypes were high. Finally, in order to further determine the association between typing results and clinical features, clinical correlation analysis was performed. Unfortunately, the results suggested that the typing was independent of ethnicity, gender and age at diagnosis (Fig. 6I).

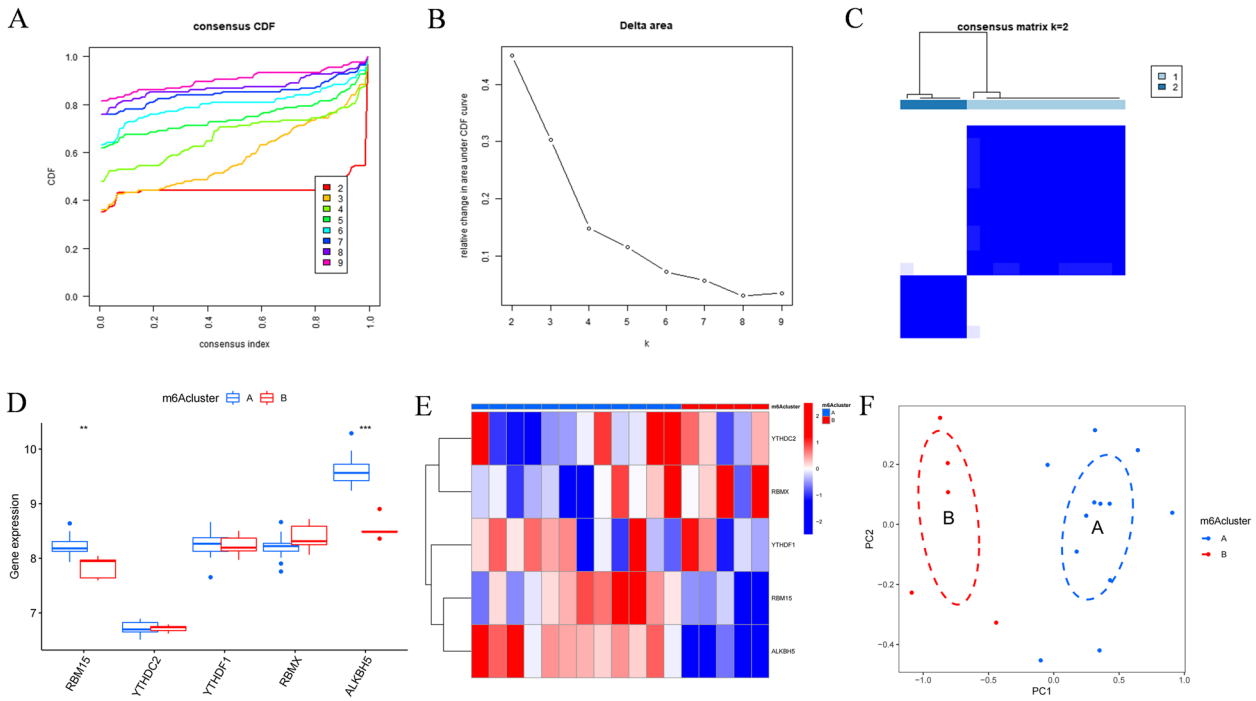


**Fig. 4** Identification and consensus clustering analysis of m6A regulators (**A**-**B**) Relative change in area under CDF curve based on results of consensus clustering for $k = 2$ to 9. **C** Consensus clustering matrix for $k = 2$. **D** Boxplot showing 2 m6A regulators with significant difference in their RNA expression between m6Acluster subtype A and B samples. **E** The heatmap of 5 m6A regulators' expression among m6Acluster subtype A and B samples. **F** PCA analysis of POAG samples. ** $p < 0.01$; *** $p < 0.001$

### Determine the m6A regulators that might be involved in the regulation of cellular biological functions of HTMCs under oxidative stress or TGF-β2 stimulation

To avoid $H_2O_2$ decay during exposure, the exposure concentration of 0.5 mM $H_2O_2$ for 1 h was selected as the optimal condition for the subsequent experiments. Next, the expression levels of the 5 differentially expressed m6A regulators obtained by bioinformatics analysis were further verified in this model, and the results suggested that the expression of YTHDC2 mRNA decreased significantly in the oxidative stress model (Fig. 7A and Supplementary Fig. 1A, beta-actin was used as the housekeeping gene in Fig. 7A-B and GAPDH was used as the housekeeping gene in Supplementary Fig. 1A-B), which was consistent with the results of bioinformatics analysis. In addtion, we also detected these genes expression levels in HTMCs treated with 5 ng/ml TGF-β2 for three days and this experiment yielded similar result that the expression of YTHDC2 mRNA decreased significantly (Fig. 7B and Supplementary Fig. 1B).

The previously mentioned results provided evidences suggesting that YTHDC2 might be involved in regulating the function of HTMCs in POAG patients. Then, transwell migration experiments confirmed that TGF-β2 stimulation caused an increase in the HTMC migration ability (Fig. 7C) and the silence of YTHDC2 showed the similar result (Fig. 7D). In addition, silencing YTHDC2 promoted the synthesis of ECM (FN, COL1A1 and ASMA) and overexpressing $YTHDC2^{WT}$ showed the reverse result. However, overexpression of $YTHDC2^{\Delta YTH}$ showed no significant changes in the synthesis of the above indexes (Fig. 7E).

## Discussion

The pathogenesis of glaucoma is quite complicated, which likely results from a combination of genetics, epigenetics, and environmental factors, and it is difficult to describe accurately with a single factor. Environmental factors can act on genomic DNA through epigenetic regulation to regulate gene expression and produce long-term phenotypic changes [22], ultimately leading to the occurrence of diseases. That is, epigenetics provides a bridge between the environment and disease [23]. For example, DNA methylation, histone modification and miRNAs participate in the pathogenesis of glaucoma by affecting the specific expression of genes related to TM and optic nerve [6–8]. It is worth noting that epigenetic changes can be reversed [24], so the application of epigenetic means to the intervention of glaucoma patients may become the future direction of glaucoma treatment. M6A

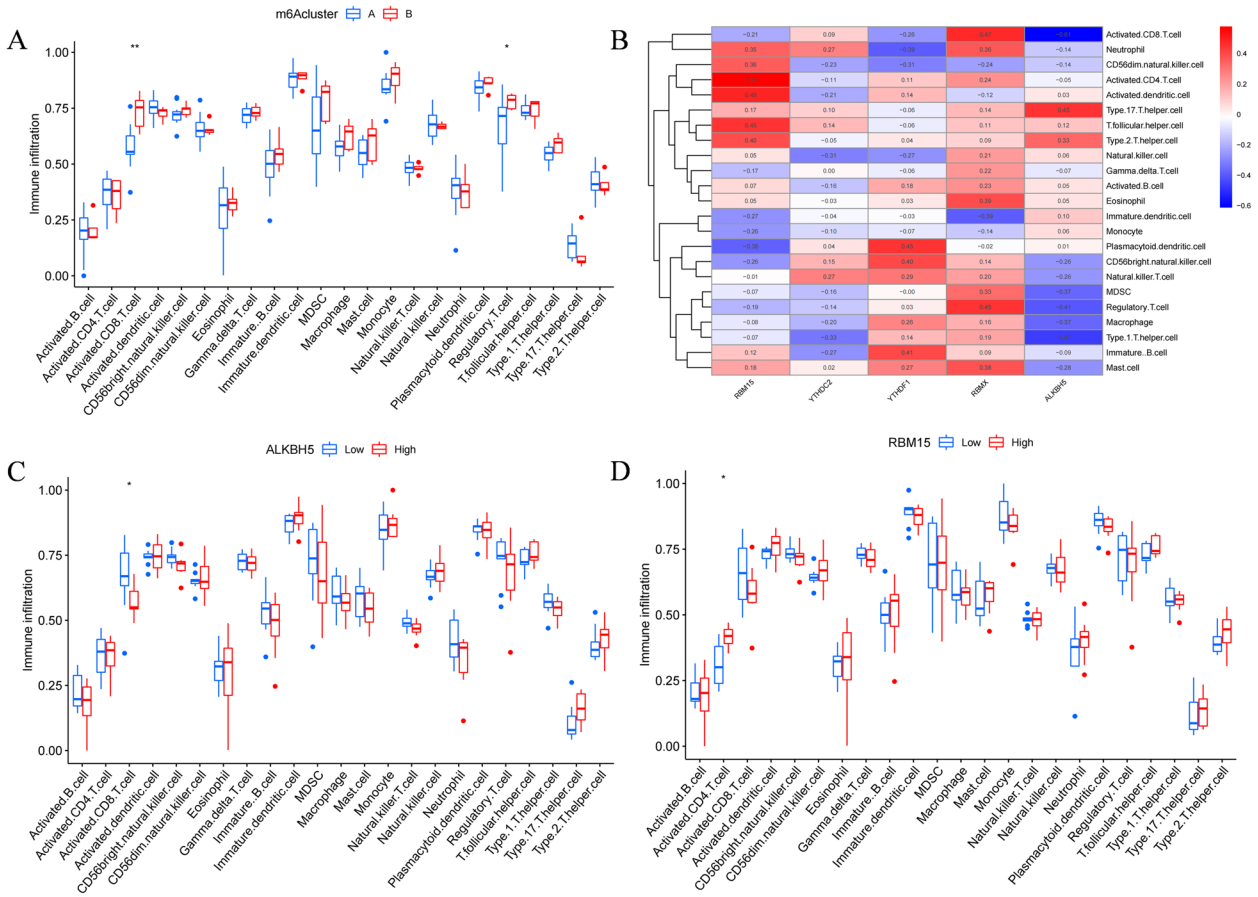


**Fig. 5** The landscape of immune cell infiltration of the two different m6A subtypes (**A**) Boxplot showing that the infiltration of 2 kinds of immune cells with significant difference between m6Acluster subtype A and B. **B** The correlation analysis of 5 differentially expressed m6A regulators with one representative class of immune cells in TM of POAG samples. **C**-**D** The infiltration of 23 kinds of immune cells between low-ALKBH5 vs. High-ALKBH5 and low-RBM15 vs. high-RBM15, respectively, in TM of POAG samples. * $p < 0.05$; ** $p < 0.01$

methylation is an important epigenetic modification mode, and emerging evidences suggest that m6A methylation plays a crucial role in the regulation of various biological processes of RNA and is involved in the pathogenesis of numerous diseases [25–28]. In recent years, some researchers began to pay attention to its important role in pseudoexfoliation glaucoma [29]. However, its role in the pathogenesis of POAG remains unclear. This study is the first attempt to investigate the role of m6A regulators in POAG.

In a first step, the expression of 25 m6A regulators in 19 normal human TM tissues and 17 human TM tissues of patients with POAG screened out from GEO datasets was analyzed. Results indicated that there were 5 differentially expressed m6A regulators in POAG samples compared to normal samples. Among 5 genes, YTHDF1 (m6A binding protein) was up-regulated, while RBM15 (m6A methyltransferase), YTHDC2 (m6A binding protein), RBMX (m6A binding protein), ALKBH5 (demethylase) were down-regulated. Further analysis showed that the importance scores of these five differentially expressed m6A regulators were all high, suggesting that these genes might play a certain role in affecting the function of TM. The molecular mechanism of action of these genes in TM of POAG patients has not yet been studied, but there have been some relevant studies in other diseases. Numerous studies have shown that these five m6A regulators depend on m6A modification to play a role in a variety of biological processes, such as proliferation, apoptosis, cell cycle regulation, migration, invasion, ECM synthesis, etc., and widely participate in the development and progression of multiple tumor or non-tumor diseases [30–35]. The dysfunction of HTMCs is known to play an important role in the pathogenesis of POAG [36–39]. Hence, it is hypothesized that the differentially expressed m6A regulators in TM tissues might be involved in the pathobiological mechanisms underlying POAG by causing cell dysfunction. And a nomogram for predicting risk of POAG using these five genes was successfully built, which further illustrated that the disorder

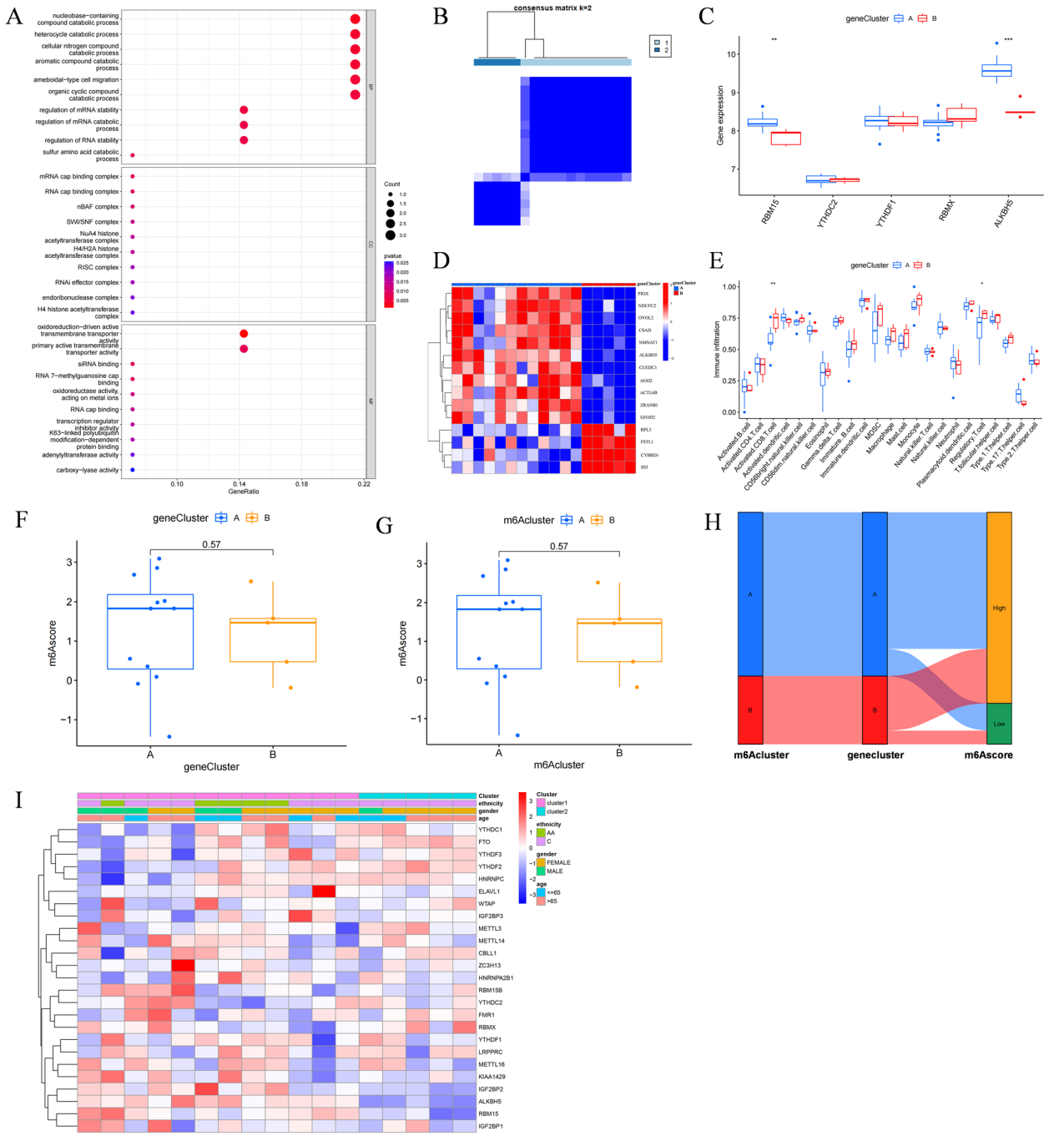


**Fig. 6** Identification and consensus clustering analysis of DEGs between the m6Acluster subtype A and B (**A**) GO enrichment analysis of the DEGs. **B** Consensus clustering matrix for k = 2. **C** Boxplot showing 2 m6A regulators with significant difference in their RNA expression between genecluster subtype A and B samples. **D** The heatmap of the DEGs' expression among genecluster subtype A and B samples. **E** Immune cell infiltration analysis in the two different gene subtypes. **F**-**G** The boxplot showing the landscape of m6A score among different m6Acluster subtypes or genecluster subtypes. **H** The Sankey diagram showing the correlations between the two types of typing and the landscape of m6A score. **I** The clinical correlation analysis showing the correlation between typing results and clinical features. * $p < 0.05$; ** $p < 0.01$; *** $p < 0.001$

of m6A regulator expression maybe cause a high risk of POAG. Therefore, it seems reasonable to infer that the levels of m6A regulators and related factors in TM of patients have potential values as novel biomarkers for the diagnosis of POAG and may be candidates for targeted therapeutic targets.

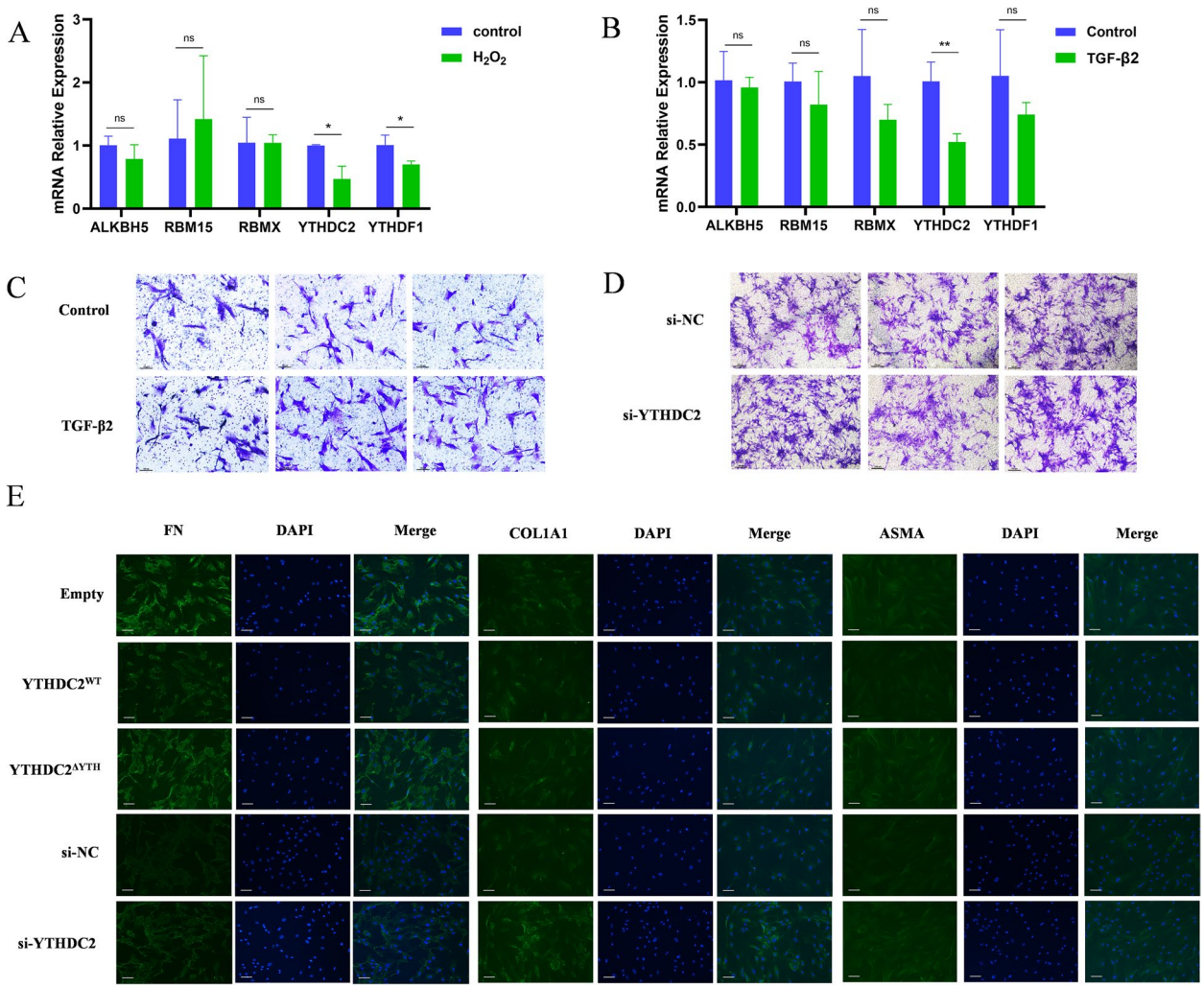


**Fig. 7** Establishment of HTMCs oxidative stress cell model and TGF-β2 stimulation cell model and search for regulating m6A related factors. **A** Expression levels of m6A related factors in oxidative stress cell model. **B** Expression levels of m6A related factors in TGF-β2 stimulation cell model. **C** Effect of TGF-β2 stimulation on HTMC migration ability. Scale bar = 100 μm. **D** Effect of YTHDC2 silence on HTMC migration ability. Scale bar = 100 μm. **E** ECM synthesis of HTMCs in different states. Scale bar = 20 μm. ** $p < 0.01$, and ns, non-significant when compared to the control group. Beta-actin was used as the housekeeping gene in Fig. 7A-B

Interestingly, the TM samples of POAG were successfully sub-classify into two groups in two ways and the typing results using these two classification methods completely coincided. This suggests that POAG patients are not all homogeneous, which is a reminder that a personalized therapeutic concept is eagerly needed. Much to our regret, no positive results were observed in further correlation analysis of typing results and clinical features. It was shown that the typing was independent of ethnicity, gender and age at diagnosis. The sample size, however, was not large enough, which could lead to the presence of false-negative results. Moreover, the GEO data set included in this study lacked detailed patient-related clinical information, such as glaucoma staging, sensitivity to IOP-lowering medications, and rate of visual field progression, which prevented further in-depth clinical analysis in this study. This suggests that when sequencing non-tumor biological samples (such as POAG), researchers should also record the clinical information of the included objects in detail, which will be more helpful to compare the personalized differences among different patients. This no doubt contributes to the development of personalized and precision medicine, and also help clinical workers to judge the prognosis of diseases. However, in clinical practice, for patients who have not undergone surgery, we do not have access to the patient's TM tissues for testing. In contrast, the determination and analysis of small molecules in aqueous

humor or blood may have more potential to be promising diagnostic markers. In addition, the tissue specimens included in this study were obtained from African American and Caucasian donors. Our research group is collecting the TM tissues of the yellow race for further study, in order to explore its general rule.

Changes in the immune microenvironment are crucial in the pathogenesis of many diseases [40]. Moreover, m6A methylation has been shown to play a part in immune regulation, such as T-cell homeostasis and differentiation, anti-tumor and anti-viral immune responses, and lipopolysaccharides-induced inflammatory responses [12]. Accumulating evidences confirm that TM interacts with the immune system in many different ways. The TM can participate in innate immune responses [41], be targeted by immune-mediated damage [42], undergo inflammation [43], and produce immunosuppressive factors [43]. Understanding these relationships is important to unravel the complex mechanisms underlying those diseases that involve dysfunction of the TM, such as glaucoma. Therefore, in order to enrich the understanding of the pathogenesis of POAG, the immune characteristics were further explored. The results of ssGSEA showed that activated $CD8^+$ T cell and regulatory T cell differed between the two subtypes. This suggested that the immune status of the TM microenvironment was different in different subtypes, and the immune system disorders might serve a function in the initiation and/or sustainment of glaucomatous TM damage in some patients. Notably, correlation analysis indicated that the ALKBH5 and RBM15 might correlate with the immune response. This was consistent with the difference in the expression of ALKBH5 and RBM15 in the two subtypes, suggesting that patients might benefit from different types of molecular idiotypic therapy.

The number of HTMCs in POAG patients is reduced [37], and the cell function is impaired [38, 39]. However, most traditional IOP-lowering medications in clinical practice either increase the outflow of aqueous humor unrelated to TM or reduce the production of aqueous humor [44], which leads to a decrease in the amount of aqueous humor passing through the avascular TM, potentially stripping the metabolites of tissues and further increasing cellular stress [45]. Therefore, there is an urgent need to develop drugs with other mechanisms of action to prevent or treat pathologic hypertension comprehensively and effectively to prevent the occurrence and progression of glaucoma. In recent years, many scholars have paid up the unity efforts for this goal, and have gained some certain results. For example, some scholars have proposed a new way to discharge aqueous humor through the lymphatic channels in the human ciliary body, namely the "uveolymatic pathway", which could be promising novel therapeutic targets in POAG [46]; Trabodenoson (INO-8875) can restore the elasticity and contractility of HTMCs by promoting the degradation of ECM debris or aged collagen, thereby remodeling the old, stiff and thickened ECM structure in TM [47]; The researches on Rho kinase inhibitor [48], EP2 receptor agonist [49], Latanoprost/Nitric oxide combination [50], small interfering RNA [51] and other novel antiglaucomatous drugs are also in full swing, which hold a promise for future clinical application. We theorize that the treatment aimed at resisting TM injury, restoring TM function, and preventing or rescuing HTMC death is closest to the restoration of aqueous humor circulation under physiological state, and more consistent with the physiological mechanism in terms of reducing IOP. Some laboratories are also exploring new therapies to regenerate HTMCs, such as stem cell transplantation [52–54], which have made some progress, but many difficulties still need to be overcome before the translation of these discoveries into clinical trials.

Several factors, such as aging, oxidative stress, genetic change, as well as environmental and endogenous factors contribute to TM damage. However, overwhelming evidence suggests that oxidative stress is considered as a major factor in such damage [55]. ROS are released after mitochondrial damage caused by various diseases, aging, oxidative stress and other stress conditions [56]. Studies have confirmed that a large number of ROS exist in aqueous humor and TM of POAG patients, confirming their long-term exposure to oxidative stress [38]. Cellular or extracellular stimuli such as oxidative stress can cause damage to TM tissues, causing inflammation and death of HTMCs, thereby reducing aqueous humor drainage and causing increased IOP, eventually leading to glaucoma [36]. Also, TGF-β is proposed as a major regulatory factor in regulating aqueous humor outflow [57]. Evidence showed that TGF-β could inhibit HTMC proliferation and then participate in the pathogenesis of glaucoma [58]. The aim of this study is to further explore the molecular mechanism of TM injury and HTMC death to offer novel understanding of the development of new therapeutic targets in POAG. In order to verify whether the 5 m6A related genes previously screened play a role in TM damage, two cell models commonly used in glaucoma studies, namely HTMC oxidative stress cell model and TGF-β2 stimulation cell model as mentioned throughout this manuscript, were constructed. Encouragingly, there were significant differences in the expression levels of YTHDC2 mRNA in both models. YTHDC2 is a m6A binding protein, which is considered to be the last member of the YTH protein family, and it identifies m6A through the YTH domain [35]. Studies have shown that YTHDC2 can

enhance the translation efficiency and decrease the mRNA abundance of its targets [59]. In recent years, the regulatory roles of YTHDC2 dependent on m6A modification in a variety of biological processes have been demonstrated, such as proliferation [60], invasion [51], metastasis [52]. For example, studies have found that the down-regulation of YTHDC2 induced by smoking promoted the proliferation and migration of lung cancer cells [60]. Moreover, our study presented that TGF-β2 stimulation caused an increase in the HTMCs migration ability and the silence of YTHDC2 showed the similar outcome. Some scholars believe that excessive proliferation and migration of HTMCs may obstruct drainage angle tissue [61]. Some researchers also believe that the decrease in cell migration ability will affect the compliance of TM, which may further reduce the outflow of aqueous humor [62]. Anyway, TGF-β2-YTHDC2 pathway may play a role in the development of POAG by regulating the migration ability of HTMCs. In addition, silencing YTHDC2 promoted the synthesis of ECM and overexpressing $YTHDC2^{WT}$ showed the reverse result. However, overexpressing $YTHDC2^{\Delta YTH}$ showed no significant changes. We know that YTHDC2 identifies m6A through the YTH domain. However, when we overexpressed YTHDC2 without YTH domain in cells, the level of the ECM synthesis did not change significantly. The above results indicate that the regulation of ECM synthesis ability by YTHDC2 may function through its YTH domain, that is, through its recognition and binding of m6A modified RNA, ultimately affect the fate of target RNA. And it's well known that oxidative stress and increased TGF-β2 are two important factors for TM dysfunction in POAG. The ECM synthesis is increased in HTMCs under oxidative stress, and TGF-β2 intervention can also play a similar role. Therefore, we speculated that there is a TGF-β2-YTHDC2 pathway in TM of POAG, and it plays a certain role in the regulation of cell function. In addition, YTHDC2 also plays a part in the altered function of HTMCs under oxidative stress.

This study provides insights into the epigenetic mechanism of TM dysfunction in POAG and provides a new possible regulatory mechanism for the mechanistic study of POAG. Our research shows that m6A regulators in TM may serve as potential diagnostic biomarkers for POAG. In addition, in HTMCs, the expression level of YTHDC2 mRNA changed under oxidative stress or TGF-β2 intervention, and then exerted its regulation on cell migration and ECM synthesis capability. The above mechanisms may be an important part of the disease process of POAG, and the specific regulatory mechanisms still need to be further explored.

## Supplementary Information

The online version contains supplementary material available at https://doi.org/10.1186/s12920-025-02123-6.

Supplementary Material 1. Figure 1. (A) Expression levels of m6A related factors in oxidative stress cell model. (B) Expression levels of m6A related factors in TGF-β2 stimulation cell model. GAPDH was used as the housekeeping gene.

**Acknowledgements**
The authors thank the study participants who make this work possible and acknowledge the research infrastructure of the Aier Glaucoma Institute, Aier Eye Institute and Aier Eye Bank.

**Commercial relationships disclosures**
None.

**Authors' contributions**
X.Y.Z. and J.W.C. carried out the design of the idea of the article and was a major contributor in writing the manuscript; X.Y.Z., D.M.Z., L.L., Y.Z. and P.W. carried out the bioinformatic analysis; F.N., Z.M.L. and Z.Y.C. assisted in the writing of the discussion section; X.C.D. was responsible for the correction and revision of the manuscript; All authors read and approved the final manuscript.

**Funding**
This work was supported by Hunan Engineering Research Center for Glaucoma with Artificial Intelligence in Diagnosis and Application of New Materials [Grant No. 2023TP2225]; Changsha Municipal Natural Science Foundation [Grant No. kq2208495]; the Natural Science Foundation of Hunan Province, China [Grant No. 2023JJ40004, 2023JJ40003, 2023JJ70014]; the Science and Technology Foundation of Aier Eye Hospital Group, China [Grant No. AR2206D4, AR2206D2, AR2206D5].

**Data availability**
Data availability statement: The data are available from the corresponding author on reasonable request.

## Declarations

**Ethics approval and consent to participate**
The study was carried out in accordance with the Declaration of Helsinki. This study was approved by the ethics committee of Changsha Aier Eye Hospital (Ethics approval No. KYPJ0010), and informed consent to participate was obtained from all of the participants.

**Consent for publication**
Not applicable.

**Competing interests**
The authors declare no competing interests.

**Author details**
[1]Hunan Engineering Research Center for Glaucoma with Artificial Intelligence in Diagnosis and Application of New Materials, Glaucoma Institute, Changsha Aier Eye Hospital, Changsha, Hunan, China. [2]Aier School of Ophthalmology, Central South University, Changsha, Hunan, China. [3]The Second Xiangya Hospital, Central South University, Changsha, Hunan, China. [4]Department of Ophthalmology, The Second Affiliated Hospital of Suzhou University, Suzhou, Jiangsu, China.

Received: 22 October 2024 Accepted: 11 March 2025
Published online: 24 March 2025

**References**


1. Bourne RRA, Flaxman SR, Braithwaite T, Cicinelli MV, Das A, Jonas JB, et al. Magnitude, temporal trends, and projections of the global prevalence of blindness and distance and near vision impairment: a systematic review and meta-analysis. Lancet Glob Health. 2017;5(9):e888–97.
2. Tham YC, Li X, Wong TY, Quigley HA, Aung T, Cheng CY. Global prevalence of glaucoma and projections of glaucoma burden through 2040: a systematic review and meta-analysis. Ophthalmology. 2014;121(11):2081–90.
3. Rosenthal J, Leske MC. Open-angle glaucoma risk factors applied to clinical area. J Am Optom Assoc. 1980;51(11):1017–24.
4. Zhavoronkov A, Izumchenko E, Kanherkar RR, Teka M, Cantor C, Manaye K, et al. Pro-fibrotic pathway activation in trabecular meshwork and lamina cribrosa is the main driving force of glaucoma. Cell Cycle. 2016;15(12):1643–52.
5. Boland MV, Ervin AM, Friedman DS, Jampel HD, Hawkins BS, Vollenweider D, et al. Comparative effectiveness of treatments for open-angle glaucoma: a systematic review for the U.S. Preventive services task force. Ann Intern Med. 2013;158(4):271–9.
6. Mao W, Rubin JS, Anoruo N, Wordinger RJ, Clark AF. SFRP1 promoter methylation and expression in human trabecular meshwork cells. Exp Eye Res. 2012;97(1):130–6.
7. Bermudez JY, Webber HC, Patel GC, Liu X, Cheng YQ, Clark AF, et al. HDAC inhibitor-mediated epigenetic regulation of glaucoma-associated TGFbeta2 in the trabecular meshwork. Invest Ophthalmol Vis Sci. 2016;57(8):3698–707.
8. Wang L, Yu T, Zhang X, Cai X, Sun H. Network integration analysis and immune infiltration analysis reveal potential biomarkers for primary open-angle glaucoma. Front Cell Dev Biol. 2021;9:793638.
9. Nachtergaele S, He C. Chemical Modifications in the Life of an mRNA Transcript. Annu Rev Genet. 2018;52:349–72.
10. Wang T, Kong S, Tao M, Ju S. The potential role of RNA N6-methyladenosine in Cancer progression. Mol Cancer. 2020;19(1):88.
11. Zhao BS, Roundtree IA, He C. Post-transcriptional gene regulation by mRNA modifications. Nat Rev Mol Cell Biol. 2017;18(1):31–42.
12. Zhang C, Fu J, Zhou Y. A review in research progress concerning m6A methylation and immunoregulation. Front Immunol. 2019;10:922.
13. Luo J, Liu H, Luan S, He C, Li Z. Aberrant regulation of mRNA m(6)A modification in cancer development. Int J Mol Sci. 2018;19(9):2515.
14. Chen XY, Zhang J, Zhu JS. The role of m(6)A RNA methylation in human cancer. Mol Cancer. 2019;18(1):103.
15. Niu F, Han P, Zhang J, She Y, Yang L, Yu J, et al. The m(6)A reader YTHDF2 is a negative regulator for dendrite development and maintenance of retinal ganglion cells. Elife. 2022;11:e75827.
16. Liu Y, Allingham RR, Qin X, Layfield D, Dellinger AE, Gibson J, et al. Gene expression profile in human trabecular meshwork from patients with primary open-angle glaucoma. Invest Ophthalmol Vis Sci. 2013;54(9):6382–9.
17. Liton PB, Luna C, Challa P, Epstein DL, Gonzalez P. Genome-wide expression profile of human trabecular meshwork cultured cells, nonglaucomatous and primary open angle glaucoma tissue. Mol Vis. 2006;12:774–90.
18. Kimura S, Tokuhisa M, Okada M. Inference of genetic networks using random forests: Assigning different weights for gene expression data. J Bioinform Comput Biol. 2019;17(4):1950015.
19. Wilkerson MD, Hayes DN. ConsensusClusterPlus: a class discovery tool with confidence assessments and item tracking. Bioinformatics. 2010;26(12):1572–3.
20. Hanzelmann S, Castelo R, Guinney J. GSVA: gene set variation analysis for microarray and RNA-seq data. BMC Bioinformatics. 2013;14:7.
21. Keller KE, Bhattacharya SK, Borras T, Brunner TM, Chansangpetch S, Clark AF, et al. Consensus recommendations for trabecular meshwork cell isolation, characterization and culture. Exp Eye Res. 2018;171:164–73.
22. Mazzio EA, Soliman KF. Basic concepts of epigenetics: impact of environmental signals on gene expression. Epigenetics. 2012;7(2):119–30.
23. Jirtle RL, Skinner MK. Environmental epigenomics and disease susceptibility. Nat Rev Genet. 2007;8(4):253–62.
24. Perri F, Longo F, Giuliano M, Sabbatino F, Favia G, Ionna F, et al. Epigenetic control of gene expression: Potential implications for cancer treatment. Crit Rev Oncol Hematol. 2017;111:166–72.
25. Cheng L, Hu Q, Wang Y, Nie W, Lu H, Zhang B, et al. Cis-regulation of an m(6)a eraser by an insertion variant associated with survival of patients with non-small cell lung carcinoma. Adv Sci (Weinh). 2024;12:e2407652.
26. Liao K, Li J, He C, Peng J. N6-methyladenosine-modified SRD5A3, identified by IGF2BP3, sustains cisplatin resistance in bladder cancer. Hum Cell. 2024;38(1):30.
27. Qiu Y, Xu Q, Xie P, He C, Li Q, Yao X, et al. Epigenetic modifications and emerging therapeutic targets in cardiovascular aging and diseases. Pharmacol Res. 2024;211: 107546.
28. Naderi N, Tavalaee M, Nasr-Esfahani MH. The epigenetic approach of varicocele: a focus on sperm DNA and m6A-RNA methylation. Hum Reprod Update. 2024;31:81.
29. Guan J, Li Z, Wumaier A, Ma Y, Xie L, Wu H, et al. Critical role of transcriptome-wide m6A methylation in the aqueous humor of patients with pseudoexfoliation glaucoma. Exp Eye Res. 2023;231: 109473.
30. Zhang Y, Liu Q, Ning J, Jiang T, Kang A, Li L, et al. The proteasome-dependent degradation of ALKBH5 regulates ECM deposition in PM(2.5) exposure-induced pulmonary fibrosis of mice. J Hazard Mater. 2022;432;128655.
31. Li H, Zhong Y, Cao G, Shi H, Liu Y, Li L, et al. METTL3 promotes cell cycle progression via m(6)A/YTHDF1-dependent regulation of CDC25B translation. Int J Biol Sci. 2022;18(8):3223–36.
32. Wang W, He Y, Zhai LL, Chen LJ, Yao LC, Wu L, et al. m(6)A RNA demethylase FTO promotes the growth, migration and invasion of pancreatic cancer cells through inhibiting TFPI-2. Epigenetics. 2022;17(12):1738–52.
33. Ma M, Wang W, Wang B, Yang Y, Huang Y, Zhao G, et al. The prognostic value of N6-methyladenosine RBM15 regulators in lung adenocarcinoma. Cell Mol Biol (Noisy-le-grand). 2022;68(1):130–9.
34. Zeng X, Chen K, Li L, Tian J, Ruan W, Hu Z, et al. Epigenetic activation of RBM15 promotes clear cell renal cell carcinoma growth, metastasis and macrophage infiltration by regulating the m6A modification of CXCL11. Free Radic Biol Med. 2022;184:135–47.
35. Yuan W, Chen S, Li B, Han X, Meng B, Zou Y, et al. The N6-methyladenosine reader protein YTHDC2 promotes gastric cancer progression via enhancing YAP mRNA translation. Transl Oncol. 2022;16: 101308.
36. Sacca SC, Gandolfi S, Bagnis A, Manni G, Damonte G, Traverso CE, et al. From DNA damage to functional changes of the trabecular meshwork in aging and glaucoma. Ageing Res Rev. 2016;29:26–41.
37. Rao A, Sahay P, Chakraborty M, Prusty BK, Srinivasan S, Jhingan GD, et al. Switch to Autophagy the Key Mechanism for Trabecular Meshwork Death in Severe Glaucoma. Clin Ophthalmol. 2021;15:3027–39.
38. Fan Y, Guo L, Wei J, Chen J, Sun H, Guo T. Effects of Salidroside on Trabecular Meshwork Cell Extracellular Matrix Expression and Mouse Intraocular Pressure. Invest Ophthalmol Vis Sci. 2019;60(6):2072–82.
39. Nair KS, Srivastava C, Brown RV, Koli S, Choquet H, Kang HS, et al. GLIS1 regulates trabecular meshwork function and intraocular pressure and is associated with glaucoma in humans. Nat Commun. 2021;12(1):4877.
40. Makowski L, Chaib M, Rathmell JC. Immunometabolism: From basic mechanisms to translation. Immunol Rev. 2020;295(1):5–14.
41. Sheng Q, Sun Y, Zhai R, Fan X, Ying Y, Liu Z, et al. Murine cytomegalovirus localization and uveitic cell infiltration might both contribute to trabecular meshwork impairment in Posner-Schlossman syndrome: Evidence from an open-angle rat model. Exp Eye Res. 2023;231: 109477.
42. Zhang D, Wu J, Zhang S, Wu J. Identification of Immune Infiltration-Related ceRNAs as Novel Biomarkers for Prognosis of Patients With Primary Open-Angle Glaucoma. Front Genet. 2022;13: 838220.
43. Yarishkin O, Phuong TTT, Vazquez-Chona F, Bertrand J, van Battenburg-Sherwood J, Redmon SN, et al. Emergent Temporal Signaling in Human Trabecular Meshwork Cells: Role of TRPV4-TRPM4 Interactions. Front Immunol. 2022;13: 805076.
44. Weinreb RN, Khaw PT. Primary open-angle glaucoma. Lancet. 2004;363(9422):1711–20.
45. Zhu W, Godwin CR, Cheng L, Scheetz TE, Kuehn MH. Transplantation of iPSC-TM stimulates division of trabecular meshwork cells in human eyes. Sci Rep. 2020;10(1):2905.
46. Yucel Y, Gupta N. Lymphatic drainage from the eye: A new target for therapy. Prog Brain Res. 2015;220:185–98.
47. Qiu TG. Trabodenoson on trabecular meshwork rejuvenation: a comprehensive review of clinical data. Expert Opin Investig Drugs. 2021;30(3):227–36.
48. Saha BC, Kumari R, Kushumesh R, Ambasta A, Sinha BP. Status of Rho kinase inhibitors in glaucoma therapeutics-an overview. Int Ophthalmol. 2022;42(1):281–94.

49. Nakakura S, Kanamori A, Fukuma Y, Wakabayashi S, Nagata Y, Adachi M. Evaluation of early medication persistence with omidenepag isopropyl, a topical selective prostaglandin EP2 agonist, in patients with glaucoma: a retrospective two-institute study. BMJ Open. 2021;11(1): e040301.
50. Radell JE, Sharma HK, Auyeung KL, Paul ME, Gagliuso DJ, Chadha N, et al. Two-Year Experience With Latanoprostene Bunod in Clinical Practice. J Glaucoma. 2021;30(9):776–80.
51. Gupta A, Kafetzis KN, Tagalakis AD, Yu-Wai-Man C. RNA therapeutics in ophthalmology - translation to clinical trials. Exp Eye Res. 2021;205: 108482.
52. Xiong S, Kumar A, Tian S, Taher EE, Yang E, Kinchington PR, et al. Stem cell transplantation rescued a primary open-angle glaucoma mouse model. Elife. 2021;10:e63677.
53. Xiong S, Xu Y, Wang Y, Kumar A, Peters DM, Du Y. alpha5beta1 Integrin Promotes Anchoring and Integration of Transplanted Stem Cells to the Trabecular Meshwork in the Eye for Regeneration. Stem Cells Dev. 2020;29(5):290–300.
54. Wang Y, Osakue D, Yang E, Zhou Y, Gong H, Xia X, et al. Endoplasmic Reticulum Stress Response of Trabecular Meshwork Stem Cells and Trabecular Meshwork Cells and Protective Effects of Activated PERK Pathway. Invest Ophthalmol Vis Sci. 2019;60(1):265–73.
55. Alvarado J, Murphy C, Juster R. Trabecular meshwork cellularity in primary open-angle glaucoma and nonglaucomatous normals. Ophthalmology. 1984;91(6):564–79.
56. Rahal A, Kumar A, Singh V, Yadav B, Tiwari R, Chakraborty S, et al. Oxidative stress, prooxidants, and antioxidants: the interplay. Biomed Res Int. 2014;2014: 761264.
57. Prendes MA, Harris A, Wirostko BM, Gerber AL, Siesky B. The role of transforming growth factor beta in glaucoma and the therapeutic implications. Br J Ophthalmol. 2013;97(6):680–6.
58. Wang X, Huai G, Wang H, Liu Y, Qi P, Shi W, et al. Mutual regulation of the Hippo/Wnt/LPA/TGF-beta signaling pathways and their roles in glaucoma (Review). Int J Mol Med. 2018;41(3):1201–12.
59. Hsu PJ, Zhu Y, Ma H, Guo Y, Shi X, Liu Y, et al. Ythdc2 is an N(6)-methyladenosine binding protein that regulates mammalian spermatogenesis. Cell Res. 2017;27(9):1115–27.
60. Wang J, Tan L, Jia B, Yu X, Yao R, Ouyang N, et al. Downregulation of m(6)A Reader YTHDC2 promotes the proliferation and migration of malignant lung cells via CYLD/NF-kappaB pathway. Int J Biol Sci. 2021;17(10):2633–51.
61. Xu H, Zhu L, Wang Y, Bao Y. Effect of Exogenous Alpha-B Crystallin on the Structures and Functions of Trabecular Meshwork Cells. J Ophthalmol. 2018;2018:7875318.
62. Last JA, Pan T, Ding Y, Reilly CM, Keller K, Acott TS, et al. Elastic modulus determination of normal and glaucomatous human trabecular meshwork. Invest Ophthalmol Vis Sci. 2011;52(5):2147–52.


## Publisher's Note